

RESEARCH PAPER

Formulation of Glycyrrhizic Acid-based Nanocomplexes for Enhanced Anti-cancer and Anti-inflammatory Effects of Curcumin

Jihyeon Song, Jun Yeong Kim, Gayeon You, Yoon Young Kang, Jiwon Yang, and Hyejung Mok

Received: 22 July 2021 / Revised: 7 September 2021 / Accepted: 12 September 2021
© The Korean Society for Biotechnology and Bioengineering and Springer 2022

Abstract In this study, nanocomplexes composed of glycyrrhizic acid (GA) derived from the root of the licorice plant (*Glycyrrhiza glabra*) were formulated for the delivery of curcumin (CUR). Sonication of amphiphilic GA solution with hydrophobic CUR resulted in the production of nano-sized complexes with a size of 164.8 ± 51.7 nm, which greatly enhanced the solubility of CUR in aqueous solution. A majority of the CURs were released from these GA/CUR nanocomplexes within 12 h. GA/CUR nanocomplexes exhibited excellent intracellular uptake in human breast cancer cells (Michigan cancer foundation-7/multi-drug resistant cells), indicating enhanced anti-cancer effects compared to that of free CUR. In addition, GA/CUR nanocomplexes demonstrated high intracellular uptake into macrophages (RAW264.7 cells), consequently reducing the release of the pro-inflammatory cytokine tumor necrosis factor- α . Furthermore, GA/CUR nanocomplexes successfully reduced the levels of serum pro-inflammatory cytokines and splenomegaly in a rheumatoid arthritis model.

Keywords: glycyrrhizic acid, curcumin, nanocomplexes, anti-cancer, anti-inflammatory

1. Introduction

Taking into consideration the wide range of phytochemicals that have been used for combination therapies in herbal medicine, it is crucial to elucidate the mechanisms of herb-

herb interactions and herb-drug interactions [1,2]. Licorice is a popular guide drug used to harmonize different ingredients in traditional herbal medicines [3]. Glycyrrhizic acid (GA), in particular, is a major component of licorice [4]. GA, composed of glycyrrhetic acid in combination with two glucoses, is well known for its anti-inflammatory, anti-virus, anti-oxidant, and anti-cancer effects [5,6]. In addition, GA has been widely used and studied as a natural sweetener and solubilizer in the cosmetic as well as pharmaceutical industries [7]. More recently, GA has been under study as a carrier material for hydrophobic drugs, such as paclitaxel and camptothecin, owing to its amphiphilic characteristics [8].

Curcumin (CUR), derived from the rhizomes of the *Curcumin Longa L. plant*, is popularly proposed as a pleiotropic molecule due to its promising and diverse biological effects, including various anti-cancer, anti-malarial, anti-oxidant, and anti-inflammatory properties [9,10]. Despite the superior bioactivity and therapeutic potential of CUR, its poor aqueous solubility and absorption *in vivo* limit its practical application as a drug [11,12]. To overcome these limitations, nanomaterials have been developed to enhance the stability and solubility of CUR; for example, liposomes, polymer nanoparticles, exosomes, and conjugates [13,14]. However, simple formulation processes for CUR that eliminate laborious formulation steps are yet to be established.

In this study, CUR was formulated in conjunction with GA to enhance its solubility and bioavailability *in vitro* as well as *in vivo*. The solubility of CUR in aqueous solution was examined by transmission (%) and particle sizes at various GA/CUR weight ratios using a UV spectrophotometer and *via* dynamic light scattering (DLS). Similarly, the antioxidant effect of GA/CUR nanocomplexes was assessed *via* a hydrogen peroxide (H₂O₂) scavenging assay. Moreover, the anti-cancer and anti-inflammatory effects of GA/CUR nanocomplexes were evaluated in Michigan cancer foundation-7/multi-drug resistant cells (MCF-7/MDR cells)

Jihyeon Song[†], Jun Yeong Kim[†], Gayeon You, Yoon Young Kang, Jiwon Yang, Hyejung Mok[†]
Department of Bioscience and Biotechnology, Konkuk University, Seoul 05029, Korea
Tel: +82-2-450-0448; Fax: +82-2-450-0686
E-mail: hjmok@konkuk.ac.kr

[†]Jihyeon Song and Jun Yeong Kim contributed equally to this work.

and RAW264.7 macrophages, respectively. The levels of cytokines tumor necrosis factor- α (TNF- α) and interleukin-1 β (IL-1 β) in serum were quantitatively measured in a rheumatoid arthritis (RA) mouse model, following the treatment with GA/CUR nanocomplexes *in vivo*.

2. Materials and Methods

2.1. Materials

GA was purchased from Tokyo Chemical Industry Co., Ltd. (Tokyo, Japan). The following list of reagents was purchased from Sigma Aldrich (St. Louis, MO, USA): CUR, dimethyl sulfoxide (DMSO), 37% formaldehyde, ethyl alcohol (EtOH), Triton X-100 (Tx-100), hydrogen peroxide solution (H₂O₂; 30% w/w in H₂O), lipopolysaccharides (LPS) from *Pseudomonas aeruginosa* 10, complete Freund's adjuvant, kolliphor, as well as trypan blue. Dialysis membranes (molecular weight cut-off [MWCO]: 3.5 kDa) were purchased from Spectrum Laboratories Inc. (Rancho Dominguez, CA, USA). Antifade mounting medium with 4',6-diamidino-2-phenylindole was obtained from Vecta Laboratories (Burlingame, CA, USA). Dulbecco's phosphate-buffered saline (PBS) solution, Roswell Park Memorial Institute (RPMI) 1640 medium, Dulbecco's modified Eagle's medium (DMEM), trypsin/EDTA, penicillin/streptomycin, and fetal bovine serum (FBS) were purchased from Gibco BRL (Grand Island, NY, USA). Furthermore, bovine type II collagen and Terrell isoflurane were purchased from Chondrex Inc. (Redmond, WA, USA) and Piramal Critical Care, Inc. (Bethlehem, PA, USA), respectively. Mouse TNF- α enzyme-linked immunosorbent assay (ELISA) kits were purchased from BD Biosciences (Franklin Lake, NJ, USA), and mouse IL-1 β ELISA kits from R&D Systems (Minneapolis, MN, USA). The cell counting kit-8 (CCK-8) was obtained from Dojindo Molecular Technologies, Inc. (Kumamoto, Japan). All other chemicals and reagents used were of analytical grade. Finally, DBA-1/J mice (six-weeks-old, female) were purchased from Orient Bio Inc. (Seongnam, Korea).

2.2. Preparation and characterization of GA/CUR nanocomplexes

GA (10 mg) dissolved in EtOH and CUR (10 mg) in DMSO were mixed at diverse GA/CUR weight ratios (GA/CUR weight ratio = 0, 0.5, 1, 1.5, and 4), followed by the dropwise addition of samples into distilled water (DW) under sonication (Branson Digital Sonifier 450; Branson Ultrasonics, Danbury, CT, USA) in an ice bath for 10 min using 30% amplitude, pulse on 8 sec, pulse off 2 sec [15,16].

The transmission (%) of the GA/CUR nanocomplexes in 8% EtOH solution was measured at a wavelength of 600

nm using a UV-Vis spectrophotometer (Beckman Coulter DU730; Beckman Coulter, Inc., Brea, CA, USA) [17]. After various types of GA/CUR nanocomplexes were diluted with DW to a final CUR concentration of 200 μ g/mL, the hydrodynamic size of each particle was measured *via* DLS (Malvern Instruments Ltd., Malvern, UK). Subsequently, the different GA/CUR nanocomplexes were incubated for 5 min in PBS solution containing 5% Tx-100, followed by DLS at room temperature in order to evaluate the particle sizes.

2.3. Release of CUR from GA/CUR nano-complex

The release profile of CUR from GA/CUR nanocomplexes was analyzed *in vitro* using the dialysis diffusion method, as outlined in a previous study [18]. Briefly, 2 mL of freshly prepared GA/CUR nanocomplexes (GA/CUR weight ratio = 4) and CUR in DW were transferred to dialysis membranes (MWCO = 3.5 kDa) and dialyzed in 100 mL of PBS solution (pH 7.4). After different incubation times (0, 1, 3, 6, 12, 24, and 36 h) under stirring at 60 rpm, the solution in the dialysis membrane was diluted with PBS solution containing 1% Tx-100. The quantity of CUR in the solution was assessed by measuring the absorbance at a wavelength of 425 nm using a UV-Vis spectrophotometer.

2.4. H₂O₂ scavenging assay

In order to evaluate the antioxidant activity of the GA/CUR nanocomplexes, an H₂O₂ scavenging assay was performed as described in our previous study [19]. CUR and GA/CUR nanocomplexes (GA/CUR weight ratio = 4) were prepared at various CUR concentrations (0, 4, 8, 12, 16, and 20 μ g/mL) in DW. GA dissolved in EtOH was further diluted with DW at the corresponding concentrations of the GA/CUR nanocomplexes (0, 16, 32, 48, 64, and 80 μ g/mL). Each solution was subsequently mixed with H₂O₂ (20 mM) in PBS solution at a sample:H₂O₂ solution volume ratio of 1:2. Following incubation for 10 min at room temperature, the absorbance of each solution was measured at a wavelength of 230 nm using a UV-Vis spectrophotometer to quantify the remaining hydrogen peroxide. Since the absorbance of GA was detected at a wavelength of 230 nm, the correction value was obtained by subtracting the absorbance of the nanoparticle solution excluding the H₂O₂.

2.5. Anti-cancer effect of GA/CUR nanocomplexes in MCF-7/MDR cells

MCF-7/MDR cells were maintained in RPMI-1640 supplemented with 10% FBS, 100 U/mL penicillin, and 100 μ g/mL streptomycin at 37°C in a humidified atmosphere of 5% CO₂. To observe the differential uptake of GA/CUR nanocomplexes at the specific GA/CUR weight ratios of 1 and 4, MCF-7/MDR cells were seeded in 4-well plate chambers (Falcon Culture Slides; Falcon, Franklin Lakes,

NJ, USA) at a density of 2.5×10^5 cells per well 24 h prior to the treatment. Subsequently, CUR and GA/CUR nanocomplexes were prepared as described above and used to treat the cells at a CUR concentration of 25 μM (9.2 $\mu\text{g}/\text{mL}$) in serum-free medium, followed by incubation for 2 h at 37°C in a humidified atmosphere of 5% CO_2 . After washing thrice with PBS containing 5% FBS, the transfected cells were fixed with 3.7% formaldehyde in PBS solution for 10 min at room temperature. The fixed cells were subsequently washed with PBS solution for 1 min and then stained with mounting medium and covered with a cover slip. The fixed cells were visualized using an inverted fluorescence microscope (Axio200; Carl Zeiss, Land Baden-Württemberg, Germany) at an excitation wavelength of 525 nm and emission wavelength of 550 nm.

MCF-7/MDR cells were seeded in 6-well plates at a density of 5×10^5 cells per well, 24 h prior to treatment. CUR and GA/CUR nanocomplexes at a GA/CUR weight ratio of 4 were used to treat cells for 4 h at a CUR concentration of 25 μM (9.2 $\mu\text{g}/\text{mL}$), in the presence of 10% FBS. Following this treatment, cells were washed with PBS and detached *via* centrifugation at 5,000 rpm at 4°C for 10 min. The resulting cell pellet was washed thrice with PBS solution containing 5% FBS and lysed in 1% TX-100 in PBS solution for 10 min. After centrifugation of the cell lysate at 13,000 rpm at 4°C for 10 min, the fluorescence intensity (FI) of the supernatant was analyzed using a fluorescence microplate reader at excitation and emission wavelengths of 430 nm and 520 nm, respectively.

To quantify the anti-cancer effect of CUR, MCF-7/MDR cells were seeded in 24-well plates, at a density of 6×10^4 cells per well 24 h prior to the treatment. CUR and GA/CUR nanocomplexes at a GA/CUR weight ratio of 4 were added to the cells at a final CUR concentration of 10 μM . After treatment for 24 or 48 h, the viable cells were stained with 0.4% trypan blue solution in PBS solution and counted using a Bright-Line™ hemacytometer.

2.6. Cellular uptake of GA/CUR nanocomplexes in RAW264.7 cells

RAW264.7 cells (belonging to a murine macrophage cell line) were maintained in DMEM supplemented with 10% FBS, 100 U/mL penicillin, and 100 $\mu\text{g}/\text{mL}$ streptomycin at 37°C in a humidified atmosphere of 5% CO_2 , as described previously [20]. The cells were seeded in 6-well plates at a density of 6×10^5 cells per well, 24 h prior to the treatment. CUR and GA/CUR nanocomplexes were used to treat the cells for 2 h at a CUR concentration of 25 μM (9.2 $\mu\text{g}/\text{mL}$) in serum-containing medium. After the cells were collected using a scraper, the cells were spun down and the pellet was lysed in 1% TX-100 in PBS solution. This was followed by centrifugation of the cell lysate at 13,000 rpm

at 4°C for 10 min. Subsequently, the FI in the supernatant of each cell lysate was measured using a fluorescence microplate reader.

2.7. The level of TNF- α for RAW264.7 cells with GA/CUR nanocomplexes

The concentration of TNF- α in the conditioned medium of LPS-stimulated RAW264.7 cells induced *via* LPS was evaluated [21]. RAW264.7 cells were initially plated in 6-well plates at a density of 6×10^5 cells per well, 24 h prior to the treatment. Subsequently, the cells were pre-treated with CUR and GA/CUR nanocomplexes (GA/CUR weight ratio of 1.5 and 4) at a CUR concentration of 10 μM (3.7 $\mu\text{g}/\text{mL}$) for 6 h. GA (18 μM , 15 $\mu\text{g}/\text{mL}$) in complete media was used as a control. Cells were further stimulated with LPS (100 ng/mL) in fresh complete media in the presence of CUR, GA/CUR nanocomplexes, and GA. After co-treatment for 18 h, the concentration of TNF- α released in each sample was quantified using a TNF- α ELISA kit, according to the manufacturer's protocol.

2.8. Bioactivity of GA/CUR nanocomplexes *in vivo*

All animal care and experimental procedures were approved by the Animal Care Committee of Konkuk University. The RA models were prepared according to a previous study [22]. Briefly, bovine type II collagen (4 mg/mL) dissolved in 0.1 M acetic acid was homogenized on ice to block protein denaturation, followed by the dropwise addition of complete Freud's adjuvants to form a mixture with a 1:1 volume ratio. The resulting emulsion (100 μL) was intradermally injected into the tail of DBA-1/J mice (female, 6-week-old). Following the first immunization, a secondary injection of emulsion was performed on the 21st day after the initial immunization for boosting. After RA modeling, the DBA-1/J mice were randomly divided into five groups: non-treated group (normal group, NOR); RA mice treated with PBS solution (control group, CON); RA mice treated with GA bare complexes (80 mg/kg) in PBS solution (GA); RA mice treated with CUR (20 mg/kg) in PBS solution (CUR); and RA mice treated with GA/CUR nanocomplexes (GA 80 mg/kg and CUR 20 mg/kg; GA/CUR in PBS solution), according to previous studies [23]. All samples (500 μL) were freshly prepared and injected intraperitoneally every alternate day, from the 21st days post first immunization till the 45th day. Upon completion of 45 days following the initial immunization, whole mouse blood was isolated from the heart *via* cardiac puncture and the mice were then euthanized. Blood sera were subsequently isolated by centrifuging whole blood at 2,000 *g* for 15 min [24]. The levels of TNF- α and IL-1 β in the serum were quantitatively measured using mouse TNF- α and IL-1 β ELISA, respectively. Additionally, all isolated spleens and thymuses were weighed.

3. Results and Discussion

3.1. Characterization of GA/CUR nanocomplexes

In this study, to enhance the aqueous solubility of CUR, GA was complexed with CUR *via* tip sonication [25]. During sonication, CUR was homogeneously dispersed with amphiphilic GA, resulting in the formation of GA/CUR

nanocomplexes in aqueous solution through hydrophobic interactions (Fig. 1). After formulation, GA/CUR nanocomplexes were used to treat two types of cells (breast cancer cells and macrophages) to assess their anti-cancer and anti-inflammatory activities as compared to free CUR *in vitro*. Moreover, following the preparation of the RA models, GA/CUR nanocomplexes were administered

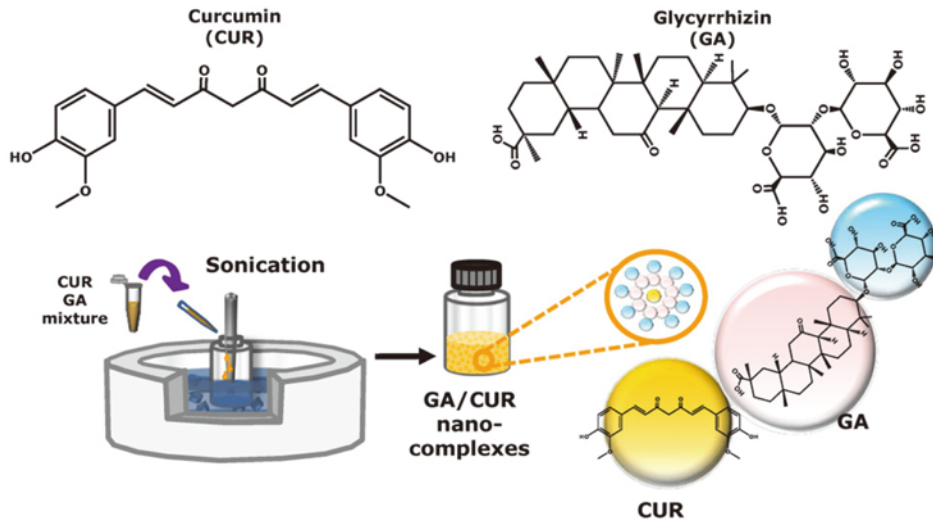


Fig. 1. Schematic illustration for the preparation of glycyrrhizic acid and curcumin (GA/CUR) nanocomplexes *via* sonication.

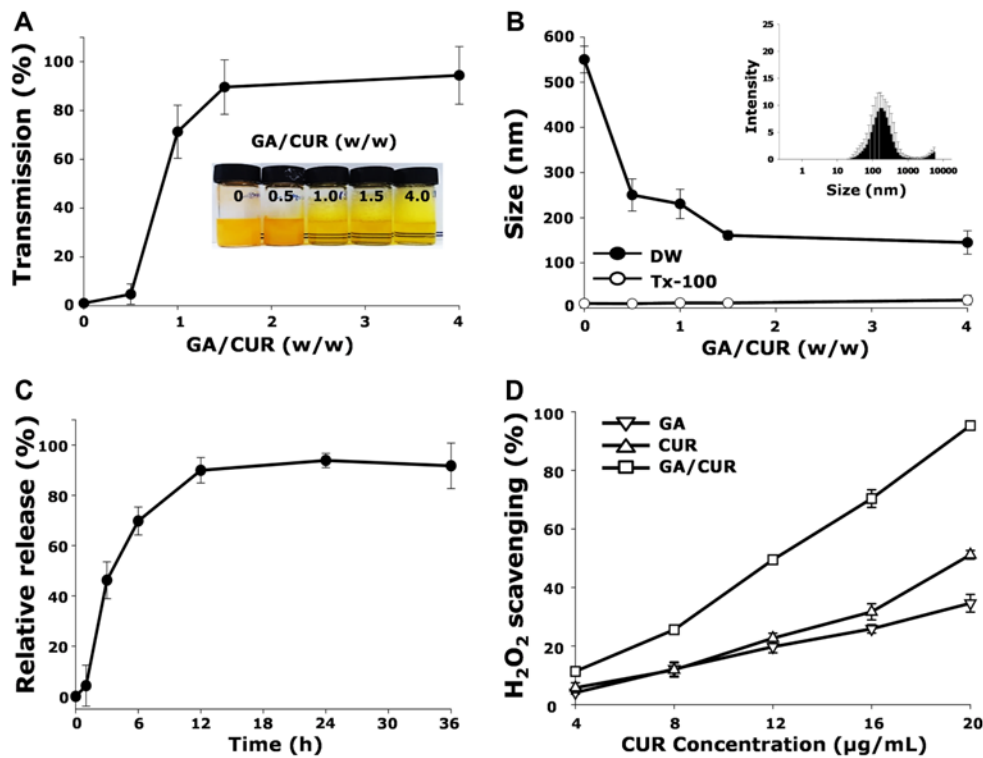


Fig. 2. (A) Transmission of glycyrrhizic acid/curcumin (GA/CUR) nanocomplexes dissolved in PBS solution measured *via* UV-spectrophotometry. (B) Hydrodynamic size of GA/CUR nanocomplexes at different GA/CUR weight ratios (inset of B: size distribution of GA/CUR nanocomplexes at GA/CUR weight ratio of 4). (C) Release assay of CUR from GA/CUR nanocomplexes. (D) H₂O₂ scavenging assay of CUR, GA, and GA/CUR nanocomplexes. PBS: phosphate-buffered saline, H₂O₂: hydrogen peroxide, DW: distilled water.

intraperitoneally to examine the anti-inflammatory effects *in vivo*.

As the weight ratio of GA/CUR increased from 0 to 4, the solubility of CUR in DW increased proportionately, as investigated by measuring the transmission (%) of the solution. Fig. 2A depicts the transmission (%) of CUR solution at a wavelength of 600 nm, after mixing CUR with GA at different GA/CUR weight ratios. While transmissions of the GA/CUR solution were below 5% at a GA/CUR weight ratio of 0.5, those at GA/CUR weight ratios of 1, 1.5, and 4 were observed to be 71.3 ± 10.9 , 89.6 ± 11.1 , and $94.4 \pm 11.8\%$, respectively. The inset in Fig. 2A presents photographic images of the GA/CUR solution at various GA/CUR weight ratios. By the formation of GA/CUR nanocomplexes, CUR was homogeneously dispersed up to 200 $\mu\text{g/mL}$ in our study. Considering that the solubility of free CUR is approximately below 11 ng/mL in aqueous solution and ~ 183.4 ng/mL in oil, GA/CUR nanocomplexes could successfully increase the solubility of CUR [12,26]. The particle sizes of the GA/CUR nanocomplexes were examined at various GA/CUR weight ratios of GA/CUR by DLS, as represented in Fig. 2B. As the GA/CUR weight ratios increased, the hydrodynamic sizes of the GA/CUR nanocomplexes decreased correspondingly. In the absence of GA, CUR exists as larger aggregates in an aqueous solution, with sizes over 500 nm. However, the size of GA/CUR nanocomplexes at a GA/CUR weight ratio of 4 was 164.8 ± 51.7 nm, with a polydispersity index of 0.3 ± 0.1 . In addition, GA/CUR nanocomplexes at a GA/CUR weight ratio of 4 showed homogeneous size distribution (inset of Fig. 2B). When GA/CUR nanocomplexes were prepared at a GA/CUR weight ratio of 4, the GA concentration was 1 mM, which is the critical micelle concentration of GA [15,27]. After incubation of GA/CUR in the presence of a surfactant (5% Tx-100 in PBS solution), no noticeable

nanoparticles were observed. This result indicates that GA/CUR nanocomplexes were formed *via* reversible noncovalent interactions; for example, hydrophobic interactions. To further examine whether free CUR could be released from GA/CUR nanocomplexes, GA/CUR nanocomplexes contained within dialysis bags (3.5 kDa) were incubated in PBS solution for predetermined time intervals, and the released CUR was measured using a UV-Vis spectrophotometer. As depicted in Fig. 2C, CUR was almost completely released (approximately 95.6%) in a sustained manner over 12 h.

3.2. H₂O₂ scavenging activity

CUR is a well-known antioxidant molecule that is crucial for its biological effects. To examine whether the antioxidant effect of GA/CUR nanocomplexes was reduced, an H₂O₂ scavenging assay was performed (Fig. 2D). GA/CUR nanocomplexes at a GA/CUR weight ratio of 4 exhibited excellent H₂O₂ scavenging activity ($95.3 \pm 1.4\%$), at a CUR concentration of 20 $\mu\text{g/mL}$. This result indicates that complexation with GA has negligible harmful effects on the antioxidant activity of CUR bioactivity. According to our previous study, CUR nano-formulation using nano-sized exosomes also produced enhanced antioxidant effects compared to free CUR [19]. It is likely that the homogeneous dispersion of CUR *via* nano-complexation might provide excellent antioxidant effects in aqueous solutions.

3.3. Anti-cancer effect of GA/CUR nanocomplexes

To examine the intracellular delivery of GA/CUR nanocomplexes, MCF-7/MDR cells were treated with CUR and GA/CUR nanocomplexes for 2 h. In our previous study, the expression levels of p-glycoprotein in MCF-7/MDR cells were higher than that in MCF-7 cells [28]. Because of the high expression of p-glycoprotein on cellular membranes,

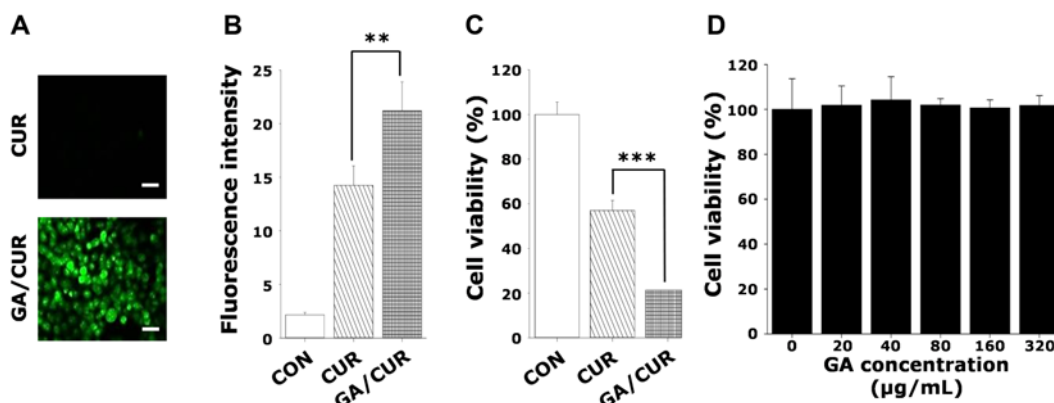


Fig. 3. (A) Inverted fluorescence microscope image of curcumin (CUR) and glycyrrhizic acid (GA)/CUR nanocomplexes in Michigan cancer foundation-7/multidrug resistant (MCF-7/MDR) cells. Scale bar: 50 μm . (B) The fluorescence intensity of CUR and GA/CUR nanocomplexes in MCF-7/MDR cells (** $p < 0.01$). (C, D) Cell viability of MCF-7/MDR cells after treatment with (C) GA/CUR nanocomplexes (***) ($p < 0.001$) and (D) GA for 24 h. CON: control.

free CUR demonstrated negligible intracellular accumulation, as depicted in Fig. 3A. However, GA/CUR nanocomplexes with a GA/CUR weight ratio of 4 exhibited much higher intracellular localization than free CUR. The amount of intracellular CUR was also quantitatively measured *via* the fluorescence intensity of CUR within cells, after incubation of the MCF-7 and MDR cells with CUR and GA/CUR nanocomplexes, respectively (Fig. 3B). Intracellular fluorescence intensities of CUR and GA/CUR were observed to be 14.3 ± 1.8 and 21.2 ± 2.7 , respectively. Fig. 3A and 3B indicate that GA/CUR nanocomplexes allowed increased intracellular localization of CUR, which might be crucial for bioactivity.

To determine the anti-cancer effect of GA/CUR nanocomplexes, cancer cell viability was assessed *via* a cell counting after treatment of the samples for 24 h. As presented in Fig. 3C, the viability of cells with CUR and GA/CUR nanocomplexes was 57.1 ± 4.4 and $21.3 \pm 4.4\%$, respectively, when compared to that of the control group (100% viability). This result indicates that the anti-cancer activity demonstrated by GA/CUR nanocomplexes was approximately 2.6-folds higher than that of CUR, which might be attributed to the increased intracellular localization of CUR. However, GA exerted negligible effects on the viability of MCF-7/MDR cells at various concentrations (Fig. 3D). Although several studies have reported the anti-cancer effects of GA in breast cancer cells, noticeable effects of GA were not observed in our results, possibly due to the multidrug-resistance of breast cancer cells [29,30].

3.4. Anti-inflammatory effect of GA/CUR nanocomplexes in macrophages

According to previous studies, CUR exhibits anti-inflammatory properties *via* the suppression of prostaglandin synthesis, which is closely related to cyclooxygenase-2 and inducible nitric oxide synthase signaling for pro-inflammatory reactions [31,32]. To assess the anti-inflammatory activity of macrophages, intracellular uptake of GA/CUR nanocomplexes was examined in RAW264.7 cells, as depicted in Fig. 4A. While cells treated with GA/CUR nanocomplexes demonstrated a fluorescence intensity of 54.8 ± 6.2 , those that underwent treatment with CUR had a fluorescence intensity of 29.5 ± 8.8 . This result clearly indicates that the GA/CUR nanocomplexes could be efficiently delivered into the macrophages. Furthermore, in order to investigate the anti-inflammatory effects of GA/CUR nanocomplexes, RAW264.7 cells were treated with LPS at a concentration of 100 ng/mL for 18 h *in vitro* to activate inflammatory responses for macrophages, as described in a previous study [21]. After pre-treatment of the GA/CUR nanocomplexes and CUR only for a duration of 6 h, the same were treated with LPS at a concentration of 100 ng/mL for

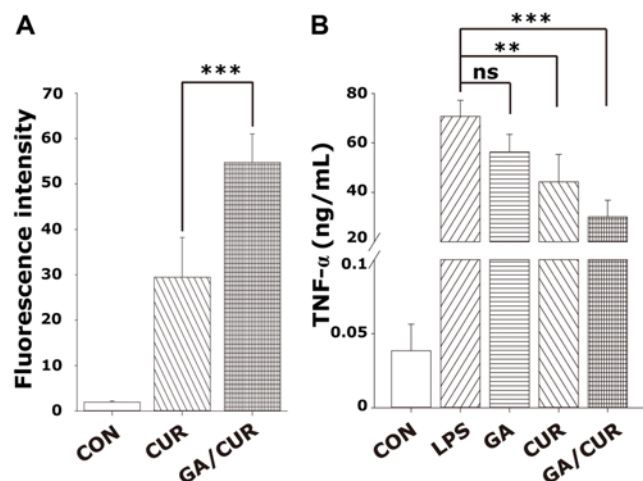


Fig. 4. (A) Intracellular uptake of curcumin (CUR) and glycyrrhizic acid (GA)/CUR nanocomplexes in RAW264.7 cells. (B) The levels of tumor necrosis factor- α (TNF- α) released in RAW264.7 cells after treatment with CUR and GA/CUR nanocomplexes in the presence of lipopolysaccharides (LPS) (100 ng/mL) (** $p < 0.01$, *** $p < 0.001$). ns: not significant, CON: control.

18 h. The level of inflammatory responses was quantitatively assessed by measuring the amount of released TNF- α , a representative pro-inflammatory cytokine, using ELISA (Fig. 4B). The concentration of released TNF- α from cells treated with CUR and GA/CUR nanocomplexes was observed to be 44.3 ± 11.1 and 30.1 ± 6.8 ng/mL, respectively, at a CUR concentration of 10 μ M, while the cytokine level in cells treated with LPS only was 70.8 ± 6.4 ng/mL.

3.5. Anti-inflammatory effects of GA/CUR nanocomplexes *in vivo*

In previous studies, CUR and GA exhibited anti-rheumatoid effects *in vivo* that were correlated to their anti-inflammatory activity *in vivo* [33]. To determine the anti-inflammatory effects of GA/CUR nanocomplexes, a collagen-induced RA mouse model was prepared by intradermal administration of bovine type II collagen and complete Freund's adjuvants (Fig. 5A). Following the 13 times injection of GA/CUR nanocomplexes at concentration of 20 mg/kg of CUR every alternate day, sera of all mice were collected on the 45th day to determine the amount of pro-inflammatory cytokines, TNF- α and IL-1 β [34]. The concentration of TNF- α in blood sera was observed as follows: 3.4 ± 3.0 , 18.1 ± 6.4 , 9.7 ± 4.9 , 8.3 ± 5.4 , and 6.3 ± 4.2 pg/mL after treatment with NOR, CON, GA, CUR, and GA/CUR nanocomplexes, respectively (Fig. 5B). In addition, the levels of IL-1 β in blood sera were as follows: 1.1 ± 0.8 , 2.4 ± 0.5 , 0.9 ± 1.0 , 3.1 ± 0.8 , and 1.2 ± 0.8 pg/mL after treatment with NOR, CON, GA, CUR, and GA/CUR nanocomplexes, respectively (Fig. 5C). These results clearly indicate that GA/CUR nanocomplexes greatly reduced

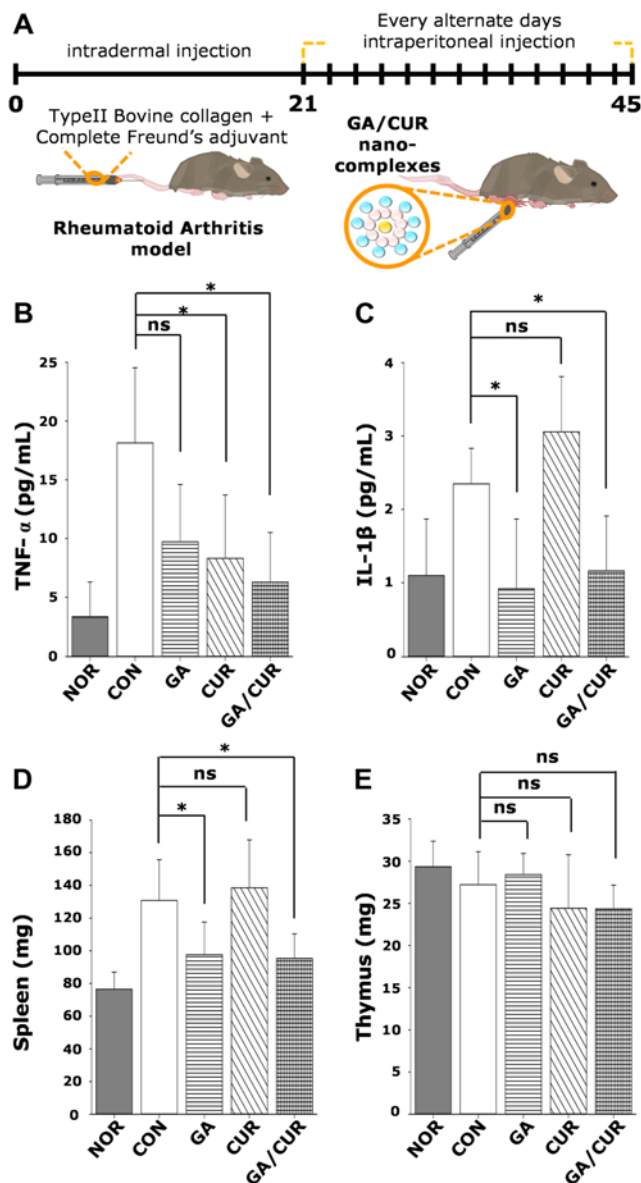


Fig. 5. (A) Schematic illustration for *in vivo* administration of glycyrrhizic acid/curcumin (GA/CUR) nanocomplexes in the rheumatoid arthritis (RA) mouse model. (B, C) The extent of released (B) tumor necrosis factor- α (TNF- α) and (C) interleukin-1 β (IL-1 β) levels in serum (* $p < 0.05$). (D, E) The weight of (D) spleen and (E) thymus after administration of nanocomplexes, followed by biopsy ($n = 5-6$). NOR: normal, CON: control, ns: not significant.

TNF- α as well as IL-1 β levels in the RA model, which suggests that GA/CUR nanocomplexes produce enhanced anti-inflammatory effects in the RA model, as compared to CUR alone. Furthermore, splenomegaly and thymus enlargement observed in the RA model are sometimes used as indicators of rheumatoid arthritis [35]. The weights of spleen were 76.5 ± 10.5 , 130.8 ± 25.0 , 97.6 ± 20.0 , 138.6 ± 29.4 , and 95.3 ± 15.0 mg in the mice treated with NOR, CON, GA, CUR, and GA/CUR, respectively (Fig. 5D).

While CON and CUR groups possessed enlarged spleens, the spleen sizes in the GA and GA/CUR groups were similar to that of the NOR group. However, there were no noticeable differences in the weight of the thymus in any of the groups (Fig. 5E). This result suggests that GA/CUR nanocomplexes can reduce inflammation *in vivo* without producing any side effects, such as splenomegaly [36].

4. Conclusion

This study demonstrated the formulation and application of a GA-based nano-complex as a simple and facile carrier for CUR, both *in vitro* and *in vivo*. GA/CUR nanocomplexes with a size of 164.8 ± 51.7 nm exhibited promising antioxidant activity and anti-cancer activity in MCF-7/MDR cells, along with anti-inflammatory activity in RAW264.7 cells *in vitro*. The same could potentially be attributed to increased aqueous solubility. In the RA mouse model, GA/CUR nanocomplexes revealed remarkably reduced release of inflammatory cytokines (TNF- α and IL-1 β) after intraperitoneal administration, without any splenomegaly. Taken together, GA/CUR nanocomplexes could serve as a promising delivery system for CUR with improved *in vivo* activity and safety.

Acknowledgements

This study was supported by a grant (NRF-2020R1A2B5B01001677) from the National Research Foundation funded by the Ministry of Education, Science, and Technology, Korea.

Ethical Statements

The authors declare no conflict of interest. Neither ethical approval nor informed consent was required for this study.

References

- Zhou, X., S. W. Seto, D. Chang, H. Kiat, V. Razmovski-Naumovski, K. Chan, and A. Bensoussan (2016) Synergistic effects of Chinese herbal medicine: a comprehensive review of methodology and current research. *Front. Pharmacol.* 7: 201.
- Jermimi, M., J. Dubois, P. Y. Rodondi, K. Zaman, T. Buclin, C. Csajka, A. Orcurto, and L. E. Rothuizen (2019) Complementary medicine use during cancer treatment and potential herb-drug interactions from a cross-sectional study in an academic centre. *Sci. Rep.* 9: 5078.
- Wang, X., H. Zhang, L. Chen, L. Shan, G. Fan, and X. Gao (2013) Liquorice, a unique "guide drug" of traditional Chinese medicine: a review of its role in drug interactions. *J. Ethnopharmacol.* 150: 781-790.

4. Song, W., X. Qiao, K. Chen, Y. Wang, S. Ji, J. Feng, K. Li, Y. Lin, and M. Ye (2017) Biosynthesis-based quantitative analysis of 151 secondary metabolites of licorice to differentiate medicinal *Glycyrrhiza* species and their hybrids. *Anal. Chem.* 89: 3146-3153.
5. Tong, T., H. Hu, J. Zhou, S. Deng, X. Zhang, W. Tang, L. Fang, S. Xiao, and J. Liang (2020) Glycyrrhizic-acid-based carbon dots with high antiviral activity by multisite inhibition mechanisms. *Small.* 16: e1906206.
6. Zhao, Z., Y. Xiao, L. Xu, Y. Liu, G. Jiang, W. Wang, B. Li, T. Zhu, Q. Tan, L. Tang, H. Zhou, X. Huang, and H. Shan (2021) Glycyrrhizic acid nanoparticles as antiviral and anti-inflammatory agents for COVID-19 treatment. *ACS Appl. Mater. Interfaces.* 13: 20995-21006.
7. Ming, L. J. and A. C. Y. Yin (2013) Therapeutic effects of glycyrrhizic acid. *Nat. Prod. Commun.* 8: 415-418.
8. Selyutina, O. Y. and N. E. Polyakov (2019) Glycyrrhizic acid as a multifunctional drug carrier - from physicochemical properties to biomedical applications: a modern insight on the ancient drug. *Int. J. Pharm.* 559: 271-279.
9. Abdollahi, E., A. A. Momtazi, T. P. Johnston, and A. Sahebkar (2018) Therapeutic effects of curcumin in inflammatory and immune-mediated diseases: a nature-made jack-of-all-trades? *J. Cell. Physiol.* 233: 830-848.
10. Rauf, A., M. Imran, I. E. Orhan, and S. Bawazeer (2018) Health perspectives of a bioactive compound curcumin: a review. *Trends Food Sci. Technol.* 74: 33-45.
11. Kharat, M. and D. J. McClements (2019) Recent advances in colloidal delivery systems for nutraceuticals: a case study - Delivery by Design of curcumin. *J. Colloid Interface Sci.* 557: 506-518.
12. Stohs, S. J., O. Chen, S. D. Ray, J. Ji, L. R. Bucci, and H. G. Preuss (2020) Highly bioavailable forms of curcumin and promising avenues for curcumin-based research and application: a review. *Molecules.* 25: 1397.
13. Naksuriya, O., S. Okonogi, R. M. Schiffelers, and W. E. Hennink (2014) Curcumin nanoformulations: a review of pharmaceutical properties and preclinical studies and clinical data related to cancer treatment. *Biomaterials.* 35: 3365-3383.
14. Wang, Y., Y. Li, L. He, B. Mao, S. Chen, V. Martinez, X. Guo, X. Shen, B. Liu, and C. Li (2021) Commensal flora triggered target anti-inflammation of alginate-curcumin micelle for ulcerative colitis treatment. *Colloids Surf. B Biointerfaces.* 203: 111756.
15. Wang, Y., B. Zhao, S. Wang, Q. Liang, Y. Cai, F. Yang, and G. Li (2016) Formulation and evaluation of novel glycyrrhizic acid micelles for transdermal delivery of podophyllotoxin. *Drug Deliv.* 23: 1623-1635.
16. Yang, F. H., Q. Zhang, Q. Y. Liang, S. Q. Wang, B. X. Zhao, Y. T. Wang, Y. Cai, and G. F. Li (2015) Bioavailability enhancement of paclitaxel via a novel oral drug delivery system: paclitaxel-loaded glycyrrhizic acid micelles. *Molecules.* 20: 4337-4356.
17. Kharat, M., Z. Du, G. Zhang, and D. J. McClements (2017) Physical and chemical stability of curcumin in aqueous solutions and emulsions: impact of pH, temperature, and molecular environment. *J. Agric. Food Chem.* 65: 1525-1532.
18. Tima, S., S. Anuchapreeda, C. Ampasavate, C. Berkland, and S. Okonogi (2017) Stable curcumin-loaded polymeric micellar formulation for enhancing cellular uptake and cytotoxicity to FLT3 overexpressing EoL-1 leukemic cells. *Eur. J. Pharm. Biopharm.* 114: 57-68.
19. Choi, E. S., Y. Y. Kang, and H. Mok (2018) Evaluation of the enhanced antioxidant activity of curcumin within exosomes by fluorescence monitoring. *Biotechnol. Bioprocess Eng.* 23: 150-157.
20. You, G., Y. Kim, J. H. Lee, J. Song, and H. Mok (2020) Exosome-modified PLGA microspheres for improved internalization into dendritic cells and macrophages. *Biotechnol. Bioprocess Eng.* 25: 521-527.
21. Yao, Y. D., X. Y. Shen, J. Machado, J. F. Luo, Y. Dai, C. K. Lio, Y. Yu, Y. Xie, P. Luo, J. X. Liu, X. S. Yao, Z. Q. Liu, and H. Zhou (2019) Nardochinoid B inhibited the activation of RAW264.7 macrophages stimulated by lipopolysaccharide through activating the Nrf2/HO-1 pathway. *Molecules.* 24: 2482.
22. Brand, D. D., K. A. Latham, and E. F. Rosloniec (2007) Collagen-induced arthritis. *Nat. Protoc.* 2: 1269-1275.
23. Arora, R., A. Kuhad, I. P. Kaur, and K. Chopra (2015) Curcumin loaded solid lipid nanoparticles ameliorate adjuvant-induced arthritis in rats. *Eur. J. Pain.* 19: 940-952.
24. Kang, Y. Y., J. Song, J. Y. Kim, H. Jung, W. S. Yeo, Y. Lim, and H. Mok (2019) Byakangelicin as a modulator for improved distribution and bioactivity of natural compounds and synthetic drugs in the brain. *Phytomedicine.* 62: 152963.
25. Ma, Y., J. Hao, K. Zhao, Y. Ju, J. Hu, Y. Gao, and F. Du (2019) Biobased polymeric surfactant: natural glycyrrhizic acid-appended homopolymer with multiple pH-responsiveness. *J. Colloid Interface Sci.* 541: 93-100.
26. Seidi Damyeh, M., R. Mereddy, M. E. Netzel, and Y. Sultanbawa (2020) An insight into curcumin-based photosensitization as a promising and green food preservation technology. *Compr. Rev. Food Sci. Food Saf.* 19: 1727-1759.
27. Selyutina, O. Y., A. V. Mastova, E. A. Shelepova, and N. E. Polyakov (2021) pH-sensitive glycyrrhizin based vesicles for nifedipine delivery. *Molecules.* 26: 1270.
28. Kang, Y. Y., J. Y. Kim, J. Song, and H. Mok (2019) Enhanced intracellular uptake and stability of umbelliferone in compound mixtures from *Angelica gigas* in vitro. *J. Pharmacol. Sci.* 140: 8-13.
29. Cai, S., Z. Bi, Y. Bai, H. Zhang, D. Zhai, C. Xiao, Y. Tang, L. Yang, X. Zhang, K. Li, R. Yang, Y. Liu, S. Chen, T. Sun, H. Liu, and C. Yang (2020) Glycyrrhizic acid-induced differentiation repressed stemness in hepatocellular carcinoma by targeting c-Jun N-terminal kinase 1. *Front. Oncol.* 9: 1431.
30. Cai, J., S. Luo, X. Lv, Y. Deng, H. Huang, B. Zhao, Q. Zhang, and G. Li (2019) Formulation of injectable glycyrrhizic acid-hydroxycamptothecin micelles as new generation of DNA topoisomerase I inhibitor for enhanced antitumor activity. *Int. J. Pharm.* 571: 118693.
31. Wang, C. Y., T. C. Kao, W. H. Lo, and G. C. Yen (2011) Glycyrrhizic acid and 18 β -glycyrrhetic acid modulate lipopolysaccharide-induced inflammatory response by suppression of NF- κ B through PI3K p110 δ and p110 γ inhibitions. *J. Agric. Food Chem.* 59: 7726-7733.
32. Fu, Y., E. Zhou, Z. Wei, X. Song, Z. Liu, T. Wang, W. Wang, N. Zhang, G. Liu, and Z. Yang (2014) Glycyrrhizin inhibits lipopolysaccharide-induced inflammatory response by reducing TLR4 recruitment into lipid rafts in RAW264.7 cells. *Biochim. Biophys. Acta.* 1840: 1755-1764.
33. Wang, Q., C. Ye, S. Sun, R. Li, X. Shi, S. Wang, X. Zeng, N. Kuang, Y. Liu, Q. Shi, and R. Liu (2019) Curcumin attenuates collagen-induced rat arthritis via anti-inflammatory and apoptotic effects. *Int. Immunopharmacol.* 72: 292-300.
34. Williams, R. O., L. Marinova-Mutafchieva, M. Feldmann, and R. N. Maini (2000) Evaluation of TNF-alpha and IL-1 blockade in collagen-induced arthritis and comparison with combined anti-TNF-alpha/anti-CD4 therapy. *J. Immunol.* 165: 7240-7245.
35. Liu, J., Y. Liu, W. Pan, and Y. Li (2021) Angiotensin-(1-7) attenuates collagen-induced arthritis via inhibiting oxidative stress in rats. *Amino Acids.* 53: 171-181.
36. Huang, B., Q. T. Wang, S. S. Song, Y. J. Wu, Y. K. Ma, L. L. Zhang, J. Y. Chen, H. X. Wu, L. Jiang, and W. Wei (2012) Combined use of etanercept and MTX restores CD4⁺/CD8⁺ ratio and Tregs in spleen and thymus in collagen-induced arthritis. *Inflamm. Res.* 61: 1229-1239.

Publisher's Note Springer Nature remains neutral with regard to jurisdictional claims in published maps and institutional affiliations.